A New Piecewise Linear Hyperchaotic Circuit

Chunbiao Li, Julien Clinton Sprott, Wesley Thio, and Huanqiang Zhu

***Abstract*—When the polarity information in diffusionless Lorenz equations is preserved or removed, a new piecewise linear hyperchaotic system results with only signum and absolute-value nonlinearities. Dynamical equations have seven terms without any quadratic or higher order polynomials and, to our knowledge, are the simplest hyperchaotic system. Therefore, a relatively simple hyperchaotic circuit using diodes is constructed. The circuit requires no multipliers or inductors, as are present in other hyperchaotic circuits, and it has not been previously reported.**

***Index Terms*—Hyperchaos, piecewise linear, signum nonlinearity.**

I. Introduction

HYPERCHAOS was first defined by Rössler as the dynamics in a chaotic attractor with more than one positive Lyapunov exponent, which indicates that its dynamics can exhibit multidimensional expansion [1]. It is well known that chaotic signals can be used to mask the message in secure communications. Nevertheless, the chaos-masked messages are not always secure. Once intercepted, they can be extracted with signal processing techniques [2]. Fortunately, as Pecora noted [3], higher dimensional hyperchaotic systems can overcome the limitations of chaotic signals because of their increased randomness and unpredictability. Thus, hyperchaos improves security by providing more complex and less vulnerable temporal signals for secret communications; therefore, hyperchaotic circuits are considered superior to third-order chaotic circuits in engineering fields.

Most hyperchaotic systems have polynomial nonlinearities with quadratic [1], [4]–[8] or cubic terms [9] that require multipliers in the corresponding hyperchaotic circuit. Many hyperchaotic systems were designed using extensions of the Lorenz and Rössler systems [1], [4]–[8] and have quadratic nonlinearities. Chlouverakis and Sprott [10] proposed what may be the algebraically simplest hyperchaotic snap system. However, it contains a fifth-order nonlinearity that requires four multipliers to realize. Tsubone and Saito [11] proposed a 4-D manifold piecewise linear system and gave a sufficient condition for hyperchaos. A 2-D return map provided the theoretical evidence for hyperchaos. They also enumerated several problems, such as the extension of the hyperchaos to a wider parameter range, controlling the hyperchaos, and the generalization of the manifold piecewise linear system.

We found that the polarity of some variables plays a key role in the dynamics. Thus, by replacing the quadratic terms with a signum and an absolute-value nonlinearity, it is possible to develop a new system that is chaotic or hyperchaotic without any quadratic nonlinearity. The signum function is physically implemented by a circuit switch, which can be realized with an IC or individual diodes. Therefore, a simple piecewise linear hyperchaotic circuit can be constructed without any multipliers. This circuit appears to be the simplest reported hyperchaotic circuit without multipliers or inductors. The structure of the modified canonical hyperchaotic circuit given in [12] seems simpler, but the use of inductors is not suitable for circuit integration and complicates the analysis since inductors rarely behave in an ideal manner. Other hyperchaotic circuits [13], [14] include even more complicated nonlinear elements.

In Section II we describe the hyperchaotic system with piecewise linear functions and its dynamical properties. In Section III the corresponding hyperchaotic circuit with a unique diode-based signum element is described. The last section provides discussion and the conclusion.

II. Hyperchaos From Piecewise Linear Functions

A. Piecewise Linear Hyperchaotic Model

Rescaling the Lorenz system as $(x, y, z) \to (\sigma x, \sigma y, \sigma z + r)$, $t \to t/\sigma$ and taking r, $\sigma \to \infty$ while $a = br/\sigma^2$ remains finite gives the diffusionless Lorenz system [15], [16] as

$$\begin{cases} \dot{x} = y - x \\ \dot{y} = -xz \\ \dot{z} = xy - a \end{cases} \tag{1}$$

which is chaotic for a wide range of single parameter a including $a = 1$. Introducing linear feedback control from an

Manuscript received August 16, 2014; accepted September 3, 2014. Date of publication September 10, 2014; date of current version December 1, 2014. This work was supported in part by the Jiangsu Overseas Research and Training Program for University Prominent Young and Middle-Aged Teachers and Presidents, the 4th 333 High-level Personnel Training Project (Su Talent [2011] No.15), and the National Science Foundation for Postdoctoral General Program and Special Founding Program of People's Republic of China (Grants 2011M500838 and 2012T50456) and Postdoctoral Research Foundation of Jiangsu Province (Grant 1002004C). This brief was recommended by Associate Editor E. Tlelo-Cuautle.

C. Li is with the School of Electronic and Information Engineering, Nanjing University of Information Science and Technology, Nanjing 210044, China (e-mail: chunbiaolee@gmail.com).

J. C. Sprott is with the Department of Physics, College of Letters and Science, University of Wisconsin–Madison, Madison, WI 53706-1390 USA (e-mail: sprott@physics.wisc.edu).

W. Thio is with the Department of Electrical and Computer Engineering, College of Engineering, The Ohio State University, Columbus, OH 43210 USA (e-mail: thio.7@osu.edu; wesley.thio@gmail.com).

H. Zhu is with the Secondary Specialized School of Nanjing–Pukou, Nanjing 210007, China (e-mail: zhuhqiang@163.com).

Color versions of one or more of the figures in this brief are available online at http://ieeexplore.ieee.org.

Digital Object Identifier 10.1109/TCSII.2014.2356912

additional variable (u) in system (1) produces a 4-D extension of system (1) [8] as

$$\begin{cases} \dot{x} = y - x \\ \dot{y} = -xz + u \\ \dot{z} = xy - a \\ \dot{u} = -by \end{cases} \tag{2}$$

which is hyperchaotic for a range of parameters such as $a = 2.7$ and $b = 0.44$.

When considering the nonlinear feedback in chaotic equations, a polynomial nonlinearity that includes quadratic terms x^2 or xy is common. Since quadratic term x^2 destroys the polarity information, it can be often replaced by an absolute-value term $|x|$, which does the same. Conversely, quadratic term xy preserves all polarity information and can be often replaced by $x\mathrm{sgn}(y)$ or $y\mathrm{sgn}(x)$. These substitutions can preserve the chaos while removing part of the amplitude information [17]. Numerical exploration shows that the chaos and the hyperchaos are preserved if the quadratic terms xz and xy in (2) are replaced with $z\mathrm{sgn}(x)$ and $|x|$, respectively, giving

$$\begin{cases} \dot{x} = y - x \\ \dot{y} = -z\mathrm{sgn}(x) + u \\ \dot{z} = |x| - a \\ \dot{u} = -by. \end{cases} \tag{3}$$

The resulting system is piecewise linear, which gives rise to several unusual and potentially useful features.

Systems (2) and (3) are equally simple with seven terms, but a in system (3) is no longer a bifurcation parameter. Rather, it is an amplitude parameter [18]–[20] that determines the magnitude of the variables and, hence, the size of the attractor; thus, it can be set to $a = 1$ without loss of generality. Such an amplitude parameter is useful for preventing the circuit from saturating and for controlling the amplitude of the output signals. This fortuitous fact is a result of the other six terms being first order in their variables; therefore, there is nothing to determine their scale other than the lone constant term.

Both systems have a rate of state space contraction equal to -1 and rotational symmetry with respect to the z-axis, as evidenced by their invariance under the coordinate transformation $(x, y, z, u) \to (-x, -y, z, -u)$; hence, they have the possibility of a symmetric pair of coexisting attractors [8]. However, the common multistability in system (2) is absent in system (3). Thus, the circuit has easily controlled and completely predictable behavior for any initial conditions.

Neither system (2) nor system (3) has equilibrium points; thus, the resulting periodic and chaotic attractors are "hidden" in the sense that they cannot be found by using an initial condition in the vicinity of an unstable equilibrium [21]–[29]. However, unlike system (2), the attractor of system (3) is globally attracting (all initial conditions approach it); thus, as a practical matter, it could be hardly less hidden. To our knowledge, no other such equilibrium-free system that is globally attracting has been reported. These are important features for the operation of the circuit; since the initial capacitor voltages do not matter, it cannot fail to oscillate, and there is no danger of it being saturated by the unbounded growth of the signals, as is typical of other chaotic circuits with finite and often small basins of attraction.

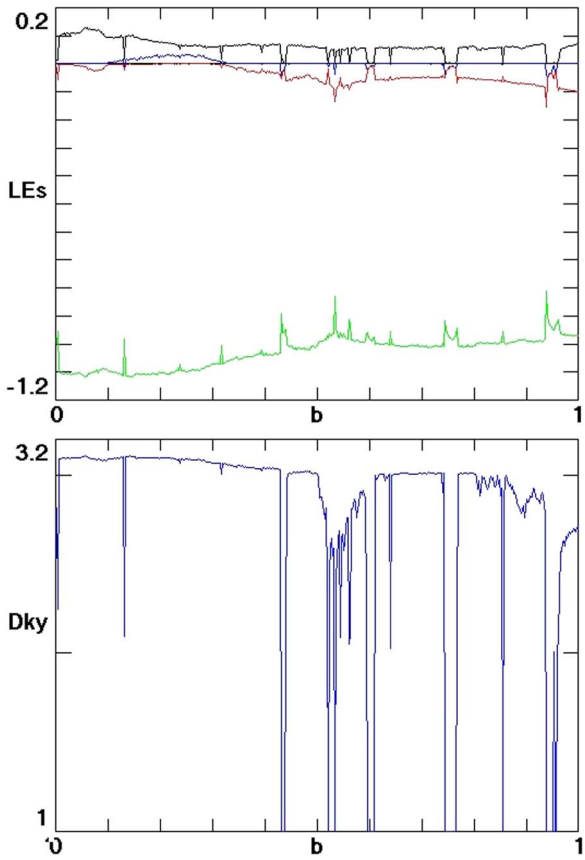

Fig. 1. Lyapunov exponents of system (3) versus b and the corresponding Kaplan–Yorke dimension.

B. Bifurcation Analysis and Maximal Hyperchaoticity

Fig. 1 shows the spectrum of the Lyapunov exponents and the corresponding Kaplan–Yorke dimension for system (3) as a function of bifurcation parameter b. The system is hyperchaotic in the approximate range of $b \in [0.1, 0.3]$, as evidenced by the two positive Lyapunov exponents. There are windows of periodicity, but the hyperchaos appears to be moderately robust (only a single narrow periodic window is evident there). At values of $b > 3.5$ (not shown), the orbit is attracted to a simple limit cycle but with a long quasi-periodic transient.

It is useful to devise a criterion for quantifying the hyperchaos to choose an optimal value of bifurcation parameter b for further detailed study. For that purpose, we use the value of b for which the second largest Lyapunov exponent divided by the most negative exponent is largest [8]. By this criterion, the hyperchaos is maximized around $b = 0.25$, where the Lyapunov exponents using the method of Wolf *et al.* [30] are (0.064, 0.033, 0, -1.098), the Kaplan–Yorke dimension is $D_{\mathrm{KY}} = 3.089$, and the correlation dimension [31] is approximately 3.01.

The corresponding signals and their power spectra are shown in Figs. 2 and 3, respectively. The time series show the rather disparate time scales that lead to the broadband power spectrum.

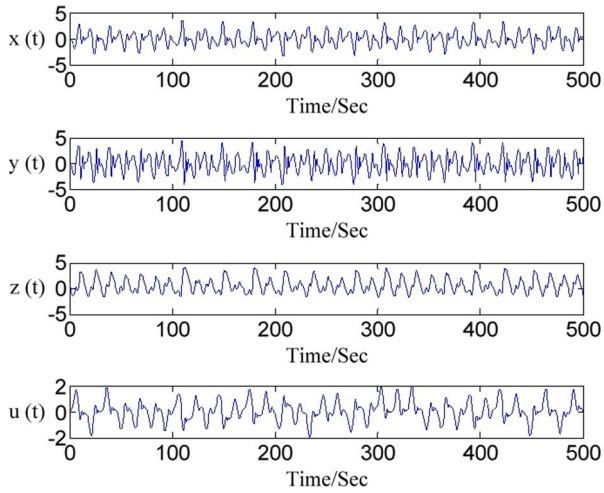

Fig. 2. Hyperchaotic signals from (3) for $a = 1$, $b = 0.25$, and initial conditions $(x_0, y_0, z_0, u_0) = (0.2, 0, 1, 0)$.

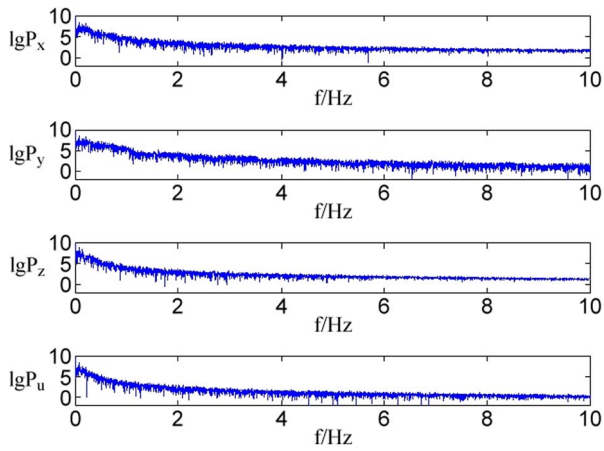

Fig. 3. Power spectrum of the signals from system (3) with $a = 1$ and $b = 0.25$.

Fig. 4 shows various projections of the hyperchaotic attractor, which resembles the attractor for the quadratic system (2) but with discontinuities in the direction of the flow vector. Although initial conditions are not critical, values of $(x, y, z, u) = (0.2, 0, 1, 0)$ are close to the hyperchaotic attractor and thus reduce the initial transient. A Poincaré section in the hyperchaotic region, as shown in Fig. 5, has a dimension greater than 2.0, indicating that the capacity dimension of the attractor is greater than 3.0.

Note that since the signum function is not continuous, the calculation of the Lyapunov exponents is problematic, as is well known [32], [33], and it is the only evidence for the hyperchaos. This problem is evident whenever none of the exponents is zero. We avoided this difficulty by replacing $\mathrm{sgn}(x)$ with $\tanh(Nx)$ and choosing $N = 250$, which is sufficiently large that the calculated exponents are independent of its value to high precision. However, this approach requires limiting the maximum temporal step size of the fourth-order adaptive Runge–Kutta integrator to 0.0005 and results in one exponent whose magnitude is everywhere less than 1×10^{-4} and is thus indistinguishable from zero in the plot in Fig. 1. Therefore, we

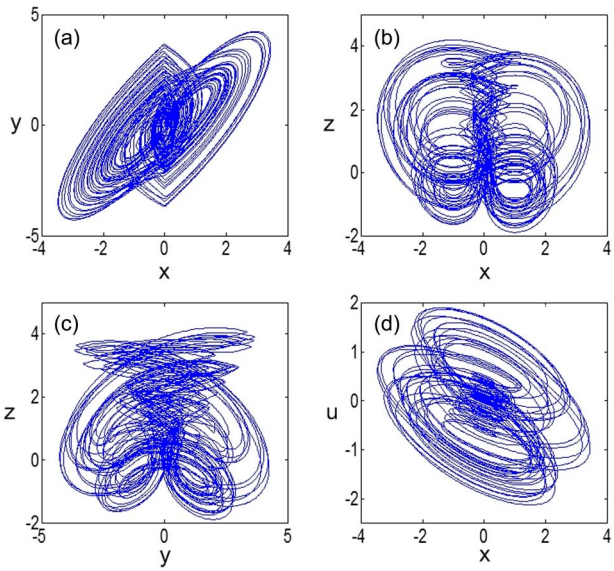

Fig. 4. Hyperchaotic attractor observed from system (3) for $a = 1$ and $b = 0.25$. (a) x–y phase plane. (b) x–z phase plane. (c) y–z phase plane. (d) x–u phase plane.

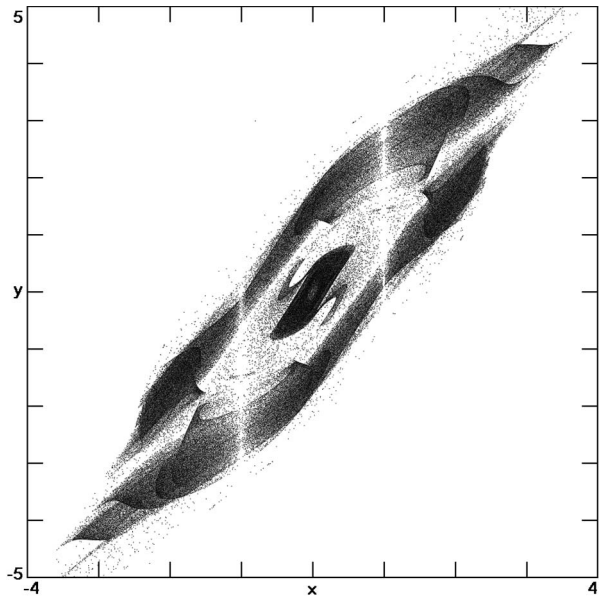

Fig. 5. Projection onto the x–y plane of a cross section of the hyperchaotic attractor at $z = 0$ for system (3) with $a = 1$ and $b = 0.25$.

are confident in the hyperchaos and in the values quoted and shown in Fig. 1.

III. Circuit Realization of Hyperchaos Without Multipliers

This section describes the design and construction of an electronic circuit that realizes system (3) using four integration channels and a unique circuit that models the signum nonlinearity. The integration channels are designed by general analog computation methods incorporated with a circuit element for the implementation of the absolute value, as shown in Fig. 6. For the nonlinearity of $z\mathrm{sgn}(x)$, the most common electronic implementation uses multipliers [34], [35], such as the example

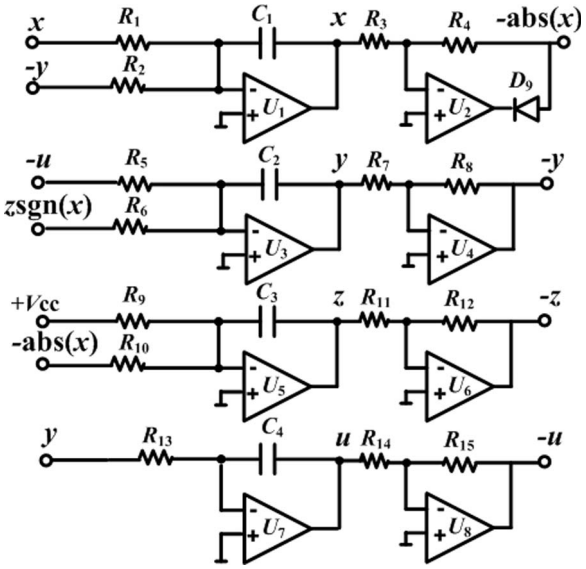

Fig. 6. Four integration channels in the circuit structure for the 4-D system (3).

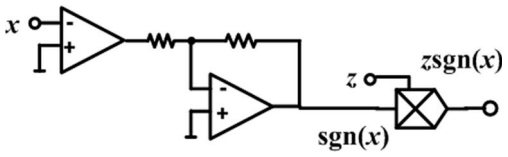

Fig. 7. Multipliers to realize the signum operation.

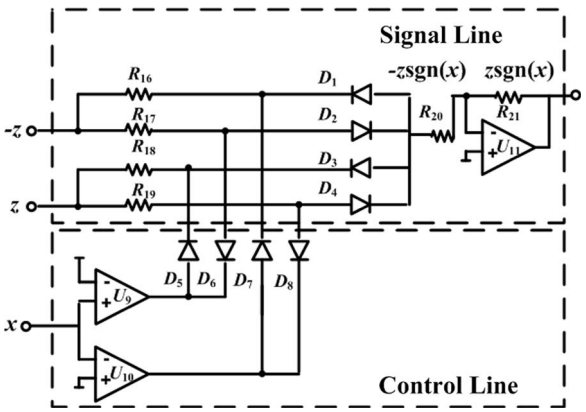

Fig. 8. Signal line and control line combined to realize the signum operation.

in Fig. 7. An alternative is to use a circuit that can switch when the polarity of a signal changes. The circuit for the implementation of $z\mathrm{sgn}(x)$ will select signal z or $-z$ depending on the polarity of x and send it to the integration channel. Such a circuit element can be constructed with a signal line and a control line, which can be built with only diodes, resistors, and a few extra operational amplifiers.

The schematic for this switching circuit is shown in Fig. 8. Signals z and $-z$ pass through a signal line and can be blocked when a voltage source is applied from a control line. Whether the control line will apply this voltage depends on the polarity of signal x. If x is positive, signal z is blocked, and $-z$ will pass through. If it is negative, then $-z$ is blocked, and z passes through. If it is zero, both signals z and $-z$ sum to zero.

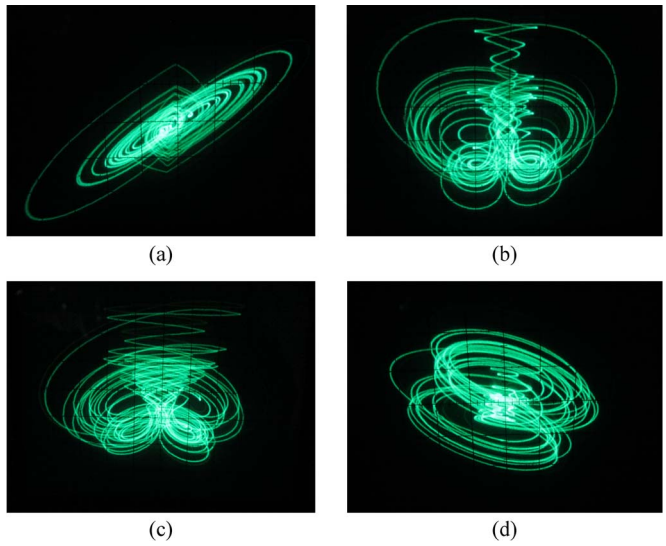

Fig. 9. Oscilloscope traces of the hyperchaotic attractors of system (3). (a) x–y plane. (b) x–z plane. (c) y–z plane. (d) x–u plane (1 V/division).

The complete circuit of Figs. 6 and 8 will produce a hyperchaotic signal. The circuit equations, where variables x, y, z, and u represent voltage levels, are given as

$$\begin{cases} \dot{x} = \frac{y}{R_2C_1} - \frac{x}{R_1C_1} \\ \dot{y} = \frac{-z\mathrm{sgn}(x)}{R_6C_2} + \frac{u}{R_5C_2} \\ \dot{z} = \frac{|x|}{R_{10}C_3} - \frac{V_{CC}}{R_9C_3} \\ \dot{u} = -\frac{y}{R_{13}C_4}. \end{cases} \tag{4}$$

Oscilloscope traces from the output of the integration channels are given in Fig. 9. The circuit parameters are $C_1 = C_2 = C_3 = C_4 = 1$ nF, $R_1 = R_2 = R_5 = R_6 = R_7 = R_8 = R_{10} = R_{11} = R_{12} = R_{14} = R_{15} = 100$ kΩ, $R_3 = R_4 = 470$ Ω, $R_9 = 900$ kΩ, $R_{13} = 400$ kΩ, and $R_{16} = R_{17} = R_{18} = R_{19} = R_{20} = R_{21} = 10$ kΩ. The operational amplifiers are TL084 ICs powered by ±9 V, and constant branch $+V_{cc}$ is powered by +9 V. Several design considerations were taken into account to prevent degrading the hyperchaotic behavior. Germanium diodes 1n60p were used to reduce the influence of the threshold voltage and crossover distortion. Silicon switching diodes such as the 1n4148 will not give an attractor that is in such close agreement with the numerical results because of their large forward voltage drop. Operational amplifier U_{11} is required to provide sufficient current to drive resistor R_6, and the resistors in the absolute-value element are required to be small for impedance matching.

The resistor values correspond to the parameters of the system and can be adjusted to change the behavior of the circuit. R_9 controls amplitude parameter a and can be a potentiometer to control the amplitude of the hyperchaotic signals. Bifurcation parameter b is controlled by R_{13} and can be adjusted between 333 kΩ and 1 MΩ to show that the system is hyperchaotic for the range of $b \in [0.1, 0.3]$.

In comparing the numerical and experimental results, the absence of the performance parameters of the active devices used in the piecewise linear model may introduce a level of inaccuracy [36]–[38]. However, the differences are not pronounced

since the hyperchaotic signals are not pushed to operate at a high frequency. This is done by keeping the capacitors at a high value. Fig. 9 shows the oscilloscope traces from this circuit in four different planes. Except for a few transients originating from different initial conditions, the result is in agreement with Fig. 4.

IV. Conclusion and Discussions

The signum function can preserve the polarity of variables in quadratic terms, whereas the absolute-value function can remove the polarity information, which produces chaos and hyperchaos with a piecewise linear nonlinearity. This approach gives rise to a new type of hyperchaotic circuit with an amplitude control knob but without any multipliers. To implement the piecewise linear selection, a new structure based on a signal line and a control line was designed to replace the multipliers and is thus simpler than other hyperchaotic circuits with multipliers and inductors. The new structure of the analog signal line and the control line designed in this brief provides a valuable circuit element for realizing signum nonlinearities. The corresponding hyperchaotic attractors show good agreement with numerical simulation.

Acknowledgment

C. Li would like to thank H. Jiang for his stimulating discussion.

References

[1] O. E. Rössler, "An equation for hyperchaos," *Phys. Lett. A*, vol. 71, no. 2/3, pp. 155–157, Apr. 1979.
[2] G. Pérez and H. A. Cerdeira, "Extracting messages masked by chaos," *Phys. Rev. Lett.*, vol. 74, no. 11, pp. 1970–1973, Mar. 1995.
[3] L. Pecora, "Hyperchaos harnessed," *Phys. World*, vol. 9, no. 5, pp. 17–18, May 1996.
[4] B. Ruy, "Dynamics of a hyperchaotic Lorenz system," *Int. J. Bifurcation Chaos*, vol. 17, no. 12, pp. 4285–4294, Dec. 2007.
[5] G. Qi, M. A. Van Wyk, B. J. Van Wyk, and G. Chen, "On a new hyperchaotic system," *Phys. Lett. A*, vol. 372, no. 2, pp. 124–136, Jan. 2008.
[6] Z. Wang, S. Cang, E. O. Ochola, and Y. Sun, "A hyperchaotic system without equilibrium," *Nonlinear Dyn.*, vol. 69, no. 1/2, pp. 531–537, Jul. 2012.
[7] Y. Li, G. Chen, and K. S. T. Wallace, "Controlling a unified chaotic system to hyperchaotic," *IEEE Trans. Circuits Syst. II, Exp. Brief*, vol. 52, no. 4, pp. 204–207, Apr. 2005.
[8] C. Li and J. C. Sprott, "Coexisting hidden attractors in a 4-D simplified Lorenz system," *Int. J. Bifurcation Chaos*, vol. 24, no. 3, pp. 1450034-1–1450034-12, Mar. 2014.
[9] Q. Li, S. Hu, S. Tang, and G. Zeng, "Hyperchaos and horseshoe in a 4D memristive system with a line of equilibria and its implementation," *Int. J. Circuits Theory Appl.,* DOI: 10.1002/cta.1912, 2013, to be published.
[10] K. E. Chlouverakis and J. C. Sprott, "Chaotic hyperjerk systems," *Chaos Solitons Fractals*, vol. 28, no. 3, pp. 739–746, May 2006.
[11] T. Tsubone and T. Saito, "Hyperchaos from a 4-D manifold piecewise-linear system," *IEEE Trans. Circuits Syst. I, Fundam. Theory Appl.*, vol. 45, no. 9, pp. 889–894, Sep. 1998.
[12] K. Thamilmaran, M. Lakshmanan, and A. Venkatesan, "Hyperchaos in a modified canonical Chua's circuit," *Int. J. Bifurcation Chaos*, vol. 14, no. 1, pp. 221–243, Jan. 2004.
[13] S. M. Yu, Z. G. Ma, S. S. Qiu, S. G. Peng, and Q. H. Lin, "Generation and synchronization of n-scroll chaotic and hyperchaotic attractors in fourth-order systems," *Chin. Phys.*, vol. 13, no. 3, pp. 317–328, Mar. 2004.
[14] D. A. Miller and G. Grassi, "Experimental realization of observer-based hyperchaos synchronization," *IEEE Trans. Circuits Syst. I, Fundam. Theory Appl.*, vol. 48, no. 3, pp. 366–374, Mar. 2001.
[15] G. van der Schrier and L. R. M. Maas, "The diffusionless Lorenz equations: Shil'nikov bifurcations and reduction to an explicit map," *Phys. D, Nonlinear Phenom.*, vol. 141, no. 1/2, pp. 19–36, Jul. 2000.
[16] J. C. Sprott, "Autonomous dissipative system," in *Elegant Chaos: Algebraically Simple Chaotic Flows*. Singapore: World Scientific, 2010, pp. 64–65.
[17] A. S. Elwakil, S. Özoğuz, and M. P. Kennedy, "Creation of a complex butterfly attractor using a novel Lorenz-Type system," *IEEE Trans. Circuits Syst. I, Fundam. Theory Appl.*, vol. 49, no. 4, pp. 527–530, Apr. 2002.
[18] C. Li and J. C. Sprott, "Chaotic flows with a single nonquadratic term," *Phys. Lett. A*, vol. 378, no. 3, pp. 178–183, Jan. 2014.
[19] C. Li and J. C. Sprott, "Amplitude control approach for chaotic signals," *Nonlinear Dyn.*, vol. 73, no. 3, pp. 1335–1341, Aug. 2013.
[20] C. Li, J. Wang, and W. Hu, "Absolute term introduced to rebuild the chaotic attractor with constant Lyapunov exponent spectrum," *Nonlinear Dyn.*, vol. 68, no. 4, pp. 575–587, Jun. 2012.
[21] G. A. Leonov and N. V. Kuznetsov, "Hidden attractors in dynamical systems from hidden oscillations in Hilbert–Kolmogov, Aizerman, Kalman problems to hidden chaotic attractors in Chua circuits," *Int. J. Bifurcation Chaos*, vol. 23, no. 1, pp. 1330002-1–1330002-69, Jan. 2013.
[22] G. A. Leonov, V. I. Vagaitsev, and N. V. Kuznetsov, "Localization of hidden Chua's attractors," *Phys. Lett. A*, vol. 375, no. 23, pp. 2230–2233, Jun. 2011.
[23] G. A. Leonov, N. V. Kuznetsov, and V. I. Vagaitsev, "Hidden attractor in smooth Chua systems," *Phys. D, Nonlinear Phenom.*, vol. 241, no. 18, pp. 1482–1486, Sep. 2012.
[24] G. A. Leonov, N. V. Kuznetsov, O. A. Kuznetsova, S. M. Seledzhi, and V. I. Vagaitsev, "Hidden oscillations in dynamical systems," *WSEAS Trans. Syst. Control*, vol. 6, no. 2, pp. 54–67, Feb. 2011.
[25] G. A. Leonov and N. V. Kuznetsov, "Algorithms for searching for hidden oscillations in the Aizerman and Kalman problems," *Dokl. Math.*, vol. 84, no. 1, pp. 475–481, Mar. 2011.
[26] N. V. Kuznetsov, G. A. Leonov, and V. I. Vagaitsev, "Analytical-numerical method for attractor localization of generalized Chua's system," in *Proc. IFAC*, 2010, pp. 29–33.
[27] N. V. Kuznetsov, O. A. Kuznetsova, G. A. Leonov, and V. I. Vagaytsev, "Hidden attractor in Chua's circuits," in *Proc. ICINCO*, 2011, pp. 279–283.
[28] G. A. Leonov and N. V. Kuznetsov, "Analytical-numerical methods for investigation of hidden oscillations in nonlinear control systems," in *Proc. IFAC*, 2011, pp. 2494–2505.
[29] N. V. Kuznetsov, G. A. Leonov, and S. M. Seledzhi, "Hidden oscillations in nonlinear control systems," in *Proc. IFAC*, 2011, pp. 2506–2510.
[30] A. Wolf, J. B. Swift, H. L. Swinney, and J. A. Vastano, "Determining Lyapunov exponents from a time series," *Phys. D, Nonlinear Phenom.*, vol. 16, no. 3, pp. 285–317, Jul. 1985.
[31] J. C. Sprott and G. Rowlands, "Improved correlation dimension calculation," *Int. J. Bifurcation Chaos*, vol. 11, no. 7, pp. 1865–1880, Jul. 2001.
[32] R. F. Gans, "When is cutting chaotic?" *J. Sound Vib.*, vol. 188, no. 1, pp. 75–83, Nov. 1995.
[33] K. Sun and J. C. Sprott, "Periodically forced chaotic system with signum nonlinearity," *Int. J. Bifurcation Chaos*, vol. 20, no. 5, pp. 1499–1507, May 2010.
[34] S. M. Yu, W. K. S. Tang, J. H. Lü, and G. Chen, "Generation of nm-Wing Lorenz-like attractors from a modified Shimizu-Morioka model," *IEEE Trans. Circuits Syst. II, Exp. Brief*, vol. 55, no. 5, pp. 1168–1172, May 2008.
[35] S. M. Yu, J. H. Lü, G. Chen, and X. H. Yu, "Design and implementation of grid multiwing butterfly chaotic attractors from a piecewise Lorenz system," *IEEE Trans. Circuits Syst. II, Exp. Brief*, vol. 57, no. 10, pp. 803–807, Oct. 2010.
[36] E. Ortega-Torres, C. Sánchez-López, and J. Mendoza-López, "Frequency behavior of saturated nonlinear function series based on opamps," *Revista Mexicana Física*, vol. 59, no. 6, pp. 504–510, Nov./Dec. 2013.
[37] E. Ortega-Torres, S. Ruíz-Hernández, and C. Sánchez-López, "Behavioral modeling for synthesizing n-scroll attractors," *IEICE Electron. Exp.*, vol. 11, no. 13, pp. 1–8, Jul. 2014.
[38] C. Sánchez-López, F. V. Fernández, V. H. Carbajal-Gómez, E. Tlelo-Cuautle, and J. Mendoza-López, "Behavioral modeling of SNFS for synthesizing multi-scroll chaotic attractors," *Int. J. Nonlinear Sci. Numer. Simul.*, vol. 14, no. 7/8, pp. 463–469, Nov. 2013.